Reprinted from **Applied Optics,** Vol. *20*, page 1676, May 1, 1981

Heterodyne frequency measurements on the 11.6-μm band of OCS: new frequency/wavelength calibration tables for 11.6- and 5.8-μm OCS bands

J. S. Wells, F. R. Petersen, A. G. Maki, and D. J. Sukle

Heterodyne difference frequency measurements between a $^{13}CO_2$ laser and a diode laser tuned (and in most cases locked) to the peaks of OCS absorption lines have been used to improve frequency calibration tables in the 860-cm^{-1} region by factors of 20–50. Measurements have been made on the vibrational transitions 10^00–00^00, 11^10–01^10, and 20^00–10^00 for OCS. The measurements on the 10^00–00^00 and 20^00–10^00 transitions are also used to provide frequency calibration tables for the 20^00–00^00 band of OCS near 1700 cm^{-1}.

I. Introduction

In an earlier paper[1] heterodyne measurements were reported for some of the frequency differences between the $2\nu_2$ absorption band of OCS (carbonyl sulfide) near 1050 cm^{-1} and the nearby CO_2 laser transitions. Since the frequencies of the CO_2 laser transitions have been measured with high accuracy,[2] such heterodyne measurements give very accurate frequencies for the OCS absorption lines. Even more recent measurements by Sattler *et al.*[3] on higher rotational transitions give further improvements in the accuracy of the OCS absorption lines near 1050 cm^{-1}. Such measurements are needed to provide convenient and accurate absorption frequency standards for the calibration of tunable laser devices, such as tunable diode lasers.

This paper reports the results of similar difference frequency measurements between $^{13}CO_2$ laser lines and the ν_1 OCS absorption lines near 870 cm^{-1}. Intensity measurements also have been made for two ν_1 OCS absorption lines. From these measurements a table of intensities and recommended frequencies (with the estimated uncertainties) is given for use in the calibration of the frequencies of tunable laser devices.

This work also gives heterodyne measurements and conventional diode laser measurements for a number of hot band absorption lines. Measurements on the 20^00–10^00 hot band yield constants which have been used to provide improved calibration tables for the 20^00–00^00 band of OCS near 1710 cm^{-1}.

An earlier paper[4] reported the results of grating and diode laser measurements on the ν_1 and $2\nu_1$ bands of OCS. That paper gave preliminary wave numbers for OCS lines from 825 to 885 cm^{-1} and from 1655 to 1737 cm^{-1}. While those tables are still useful for indicating the relative positions and intensities of some of the hot bands and isotopic species, this paper presents tables of line frequencies (and wave numbers) that are more than an order of magnitude more accurate.

II. Description of Experimental Details

Since a detailed account of our heterodyne measurement technique was presented earlier,[1] we will give only a recapitulation and indicate some recent changes. A block diagram of the experimental arrangement for our frequency measurement procedure is shown in Fig. 1. The tunable diode laser (TDL) is operated in a liquid helium Dewar which can accommodate three such devices. The chopped tunable diode laser beam goes through a monochromator, and a portion of the emerging beam is split off and goes through an OCS cell to a detector. The signal from the detector is phase detected at the chopper frequency and displayed on a recorder. In addition to the obvious functions of mode rejection and coarse calibration, the monochromator is also used to level the transmitted power as a function of frequency as the TDL scans in the vicinity of the OCS line to be measured. A flat background level allows one to use a first derivative (instead of a third derivative lock) to stabilize the diode laser to the OCS line.

D. J. Sukle is with Community College of Denver, Division of Science, Westminister, Colorado 80030; A. G. Maki is with U.S. National Bureau of Standards, Molecular Spectroscopy Division, Washington, D.C. 20234; the other authors are with U.S. National Bureau of Standards, Time & Frequency Division, Boulder, Colorado 80303.

Received 4 December 1980.

To continue on with the frequency measurement, the chopper is removed from the system, and the diode laser is frequency modulated at ~1 kHz. The phase detected signal (first derivative) is fed back to the laser control module in the proper phase to lock the diode laser frequency to the OCS line. For transitions up to $P(46)$, the $^{13}CO_2$ laser was stabilized by locking to a saturated absorption dip in low pressure (5.3-Pa or 40-mTorr) isotopic CO_2 following the scheme of Freed and Javan.[5] For $J > 46$, an unstabilized 2-m laser was carefully tuned to line center. Our frequency measurements of $P(52)$ and $P(54)$ of this laser (which contained the same laser fill pressure for all our experiments) agreed well with values (predicted for stabilized lasers) which are used in Table I.

The HgCdTe mixer used to combine these two laser signals had a 3-dB bandwidth slightly greater than 100 MHz. The heterodyne beat notes generally did not have adequate SNR for cycle counting; hence a marker from an oscillator was superposed on the heterodyne beat note and simultaneously measured on a frequency counter.

The potential accuracy of the frequency measurements depends on several factors. One factor is how

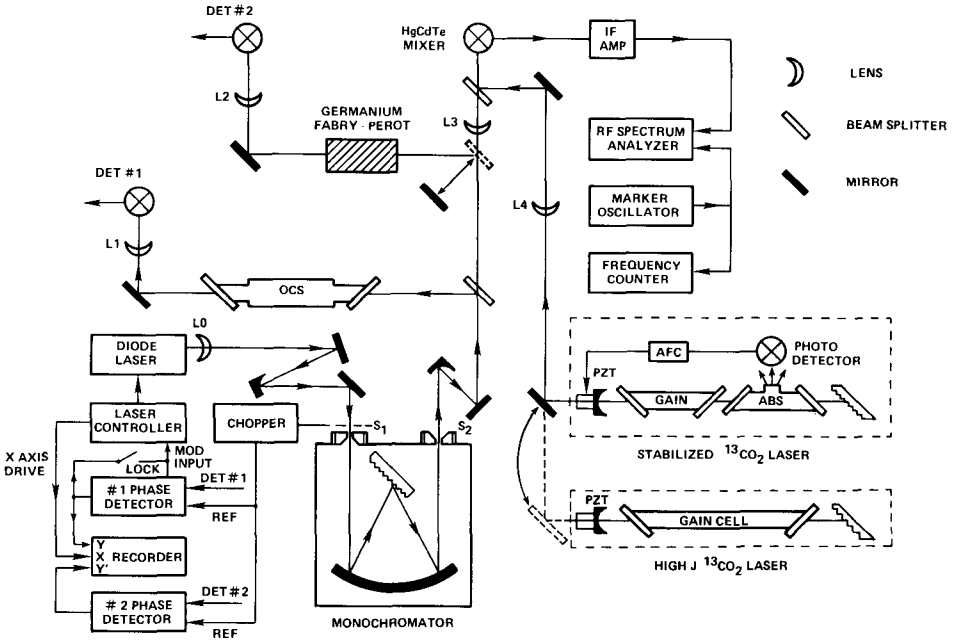

Fig. 1. Block diagram of a TDL spectrometer with capabilities for heterodyne frequency measurements with $^{13}CO_2$ lasers. A kinematically mounted mirror permits the user to select the germanium etalon for wavelength metrology or the heterodyne configuration for frequency metrology. A second mirror mount arrangement permits selection of the appropriate $^{13}CO_2$ laser.

Table I. Frequencies of 11.5-μm Band Carbonyl Sulfide Absorption Lines Measured by the Heterodyne Technique

Vibrational transition	Rot. trans.	OCS–$^{13}CO_2$ meas. freq. diff. (MHz)	Measured OCS freq. (MHz)[a]	Obs.-calc. (MHz)	CO_2 laser[b] transition	$^{13}CO_2$ freq.[c] (MHz)
10^00–00^00	$R(87)$	+73.0	26 674 291.6 (6.0)	0.4	^{13} $P(28)$	26 674 218.62
10^00–00^00	$R(75)$	+2773.8	26 566 226.9 (3.0)	−0.1	$P(32)$	26 563 453.07
10^00–00^00	$R(57)$	+395.6	26 393 239.6 (2.0)	−0.1	$P(38)$	26 392 843.97
10^00–00^00	$R(40)$	+1362.7	26 218 193.2 (3.0)	0.0	$P(44)$	26 216 830.49
10^00–00^00	$R(18)$	+1733.6	25 975 344.4 (2.0)	−1.8	$P(52)$	25 973 610.78
10^00–00^00	$R(7)$	−1668.0	25 847 177.1 (2.0)	1.5	$P(25)$	25 848 845.09[d]
10^00–00^00	$P(1)$	−1277.5	25 739 018.1 (2.0)	0.8	$P(29)$	25 740 295.57[d]
11^1e0–01^1e0	$R(84)$	+174.0	26 450 485.0 (3.0)	0.3	$P(36)$	26 450 311.04
11^1e0–01^1e0	$R(42)$	−628.4	26 034 711.5 (6.0)	0.2	$P(50)$	26 035 339.88
11^1e0–01^1e0	$R(25)$	−707.3	25 848 137.8 (2.0)	−0.7	$P(25)$	25 848 845.09[d]
11^1e0–01^1e0	$R(22)$	−1400.2	25 814 164.2 (2.0)	1.1	$P(26)$	25 815 564.36[d]
11^1f0–01^1f0	$R(42)$	+820.7	26 036 160.6 (6.0)	−1.0	$P(50)$	26 035 339.88
11^1f0–01^1f0	$R(25)$	−34.5	25 848 810.6 (4.0)	−0.2	$P(25)$	25 848 845.09[d]
11^1f0–01^1f0	$R(22)$	−841.4	25 814 723.0 (4.0)	−1.9	$P(26)$	25 815 564.36[d]
20^00–10^00	$R(86)$	+600.4	26 450 911.4 (3.0)	0.1	$P(36)$	26 450 311.04
20^00–10^00	$R(73)$	−439.6	26 334 336.9 (3.0)	−0.3	$P(40)$	26 334 776.55
20^00–10^00	$R(50)$	+810.7	26 111 131.5 (4.0)	1.2	$P(15)$	26 110 320.77[d]
20^00–10^00	$R(40)$	+85.0	26 007 511.5 (4.0)	0.0	$P(19)$	26 007 426.54[d]
20^00–10^00	$R(31)$	−329.0	25 910 930.4 (6.0)	2.3	$P(54)$	25 911 259.42
20^00–10^00	$R(16)$	+2772.1	25 743 067.7 (3.0)	−0.7	$P(29)$	25 740 295.58[d]

[a] The estimated uncertainty in megahertz is given in parentheses.
[b] A 1.25-m stabilized $^{13}CO_2$ laser was used for lines up to $P(46)$. For J above $P(46)$ and for hot band transitions, a 2-m laser was used.
[c] Except for hot band lines, laser reference frequencies were taken from Freed *et al.*[7]
[d] Recent NBS measurements of lasing $^{13}CO_2$ hot band transitions (01^11–11^10_I).

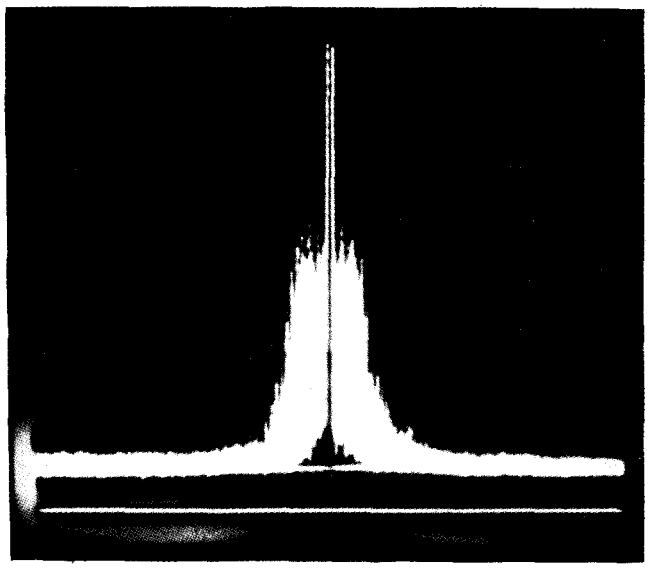

Fig. 2. Heterodyne beat note between $P(52)$ of the $^{13}CO_2$ laser and the TDL when locked to $R(30)$ of the $O^{13}CS$ molecule. The center frequency is 516.9 MHz, and the sharp feature is due to the marker oscillator. The 10-cm long spectrum analyzer trace has a 10-MHz/cm dispersion.

accurately one can determine the OCS line center. We have taken the uncertainty in finding the line center to be equal to the full width at half-maximum (FWHM) divided by the ratio of the derivative SNR. At 11 μm, the OCS FWHM is ~40 MHz. Hence a SNR of 50 will permit one to locate the line center with an uncertainty less than 1 MHz. The frequency modulation producing the derivative signal also broadens the nominal 3-MHz signal up to ~10 MHz, as shown in Fig. 2. We consider this a near ideal beat note and believe that its center can be located within 1 MHz. The narrow feature in the center is due to the marker oscillator.

Figure 3 shows the overlap of the $^{13}CO_2$ laser and the 11.6-μm OCS absorption band. The vertical lines indicate some close coincidences for potential heterodyne measurements. The solid part of the $^{13}CO_2$ laser curve represents the operable range of our 1.25-m stabilized CO_2 laser. When the $^{13}CO_2$ laser was stabilized, its frequency uncertainty was <0.2 MHz, and thus this frequency uncertainty was small compared with other possible contributions to uncertainty in the OCS frequency measurements shown in Table I. The dashed portion of the curve represents the extended range with the unstabilized 2-m higher gain laser. When the 2-m laser is used, we estimate that with great care one can tune its frequency to within ~1 or 2 MHz of the line center. For the key measurements involving the $P(29)$ hot band laser transition, the 2-m laser was stabilized with an external absorption cell.

The OCS absorption cell had a path length of 50 cm and pressures ranged from 12 Pa (0.09 Torr) for the stronger 10^00–00^00 lines to 266 Pa (2 Torr) for some of the 20^00–10^00 lines. For the weaker 20^00–10^00 lines, a 2-m absorption cell heated to 155°C was needed.

Several unexpected developments occurred during these experiments. First, the measurement of the OCS $R(18)$ line with respect to the $P(52)$ $^{13}CO_2$ laser line indicated that the frequency of $P(52)$ in the literature[6] was off considerably. New work by Freed and coworkers has verified this frequency discrepancy. Our $^{13}CO_2$ frequency values are taken from their new paper.[7] Second, our attempt to reach $P(60)$ with the 2-m laser by modifying it with a new discharge tube and high reflectivity mirror did not succeed. $P(56)$ was the limit in the new laser, and this excluded the potential measurement of $R(2)$ with respect to $P(58)$. As a result of these improvements, however, we did observe some eighteen lasing hot band (01^11–11^10_I) transitions in this region ranging from $P(10)$ to $P(30)$ and have measured their frequencies relative to the stabilized CO_2 laser.[2] These hot band measurements were made using a metal-insulator-metal or MIM diode and will be described later.[8] One hot band transition, $P(29)$, was used to obtain the only heterodyne measurement in the P branch of the OCS band.

Only a small number of lines of the OCS hot bands could be measured using the heterodyne technique because of the limited frequency response of our mixer. To cover a wider range of rotational quantum numbers and thereby improve the constants for the levels involved in the hot band transitions, we have also measured the absorption spectrum of OCS using a tunable diode laser and etalon.

For these nonheterodyne measurements, a closed cycle cooler was used, and more extensive temperature tuning of the diode was possible. A solid germanium etalon with a free spectral range of 0.0162 cm^{-1} was used to measure the wave number differences between the hot band lines and the calibration lines of the 10^00–00^00 band. The new values presented at the end of this paper were used for the calibration of these measurements. Reference 4 more clearly describes how these measurements were made. These (OCS) hot band measurements are given in Table II.

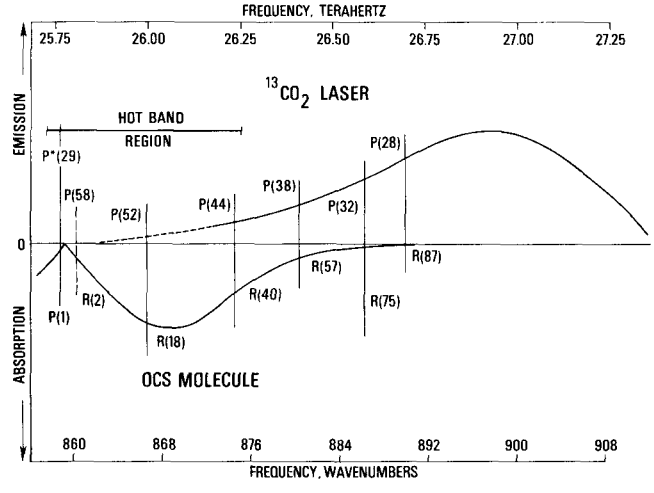

Fig. 3. Sketch of the overlap of the $^{13}CO_2$ laser emission and the 11.6-μm OCS absorption bands as a function of frequency/wave number. Only a qualitative indication of the intensities is shown in order to better illustrate the extent of the bands.

III. Results and Analysis of the Data

Table I gives the results of the present heterodyne measurements. In addition to the measured frequency differences and the derived frequencies of the OCS lines, Table I also gives the frequencies for the $^{13}CO_2$ laser transitions determined by the most recent work.[7,8]

The assignment of the measured OCS lines was fairly straightforward. The mode selecting monochromator was calibrated so that the central frequency of a given diode scan was known to within about $\pm 0.10\ cm^{-1}$. The tables given in Ref. 4 and also calculations provided by Fayt[9] were extremely useful for assigning lines through pattern recognition, i.e., by taking into account frequency separations and relative intensities. When needed for line identification, solid germanium etalons with fringe spacings (free spectral ranges) of 0.017 or $0.05\ cm^{-1}$ were used to measure approximate frequency differences.

When it was suspected that an absorption line was due to one of the isotopes ($^{18}O^{12}C^{32}S$, $^{16}O^{13}C^{32}S$, or $^{16}O^{12}C^{34}S$), the spectrum of an enriched sample was recorded to verify the assignment. In this way a few measured lines were shown to be due to $^{16}O^{13}C^{32}S$, although the vibrational assignment could not always be determined (further measurements on isotopic species will be the subject of a future paper).

To analyze the two $l = 0$ vibrational transitions, 10^00–00^00 and 20^00–10^00, we used the term value expression:

$$T(v,J) = F(v) + B_vJ(J+1) - D_vJ^2(J+1)^2 + H_vJ^3(J+1)^3, \quad (1)$$

$$\nu_0(v' \leftarrow v'') = F(v') - F(v''). \quad (2)$$

In addition to the heterodyne measurements reported in Table I, the analysis included appropriate microwave measurements taken from Refs. 10 and 11. The analysis of the 20^00–10^00 band also included diode measurements calibrated against the 10^00–00^00 lines (using Table III) and given in Table II. A least squares analysis of the data was performed with each datum given a weight inversely proportional to the square of the estimated uncertainty. The uncertainties assigned to each measurement are given in Tables I and II.

Table II. Hot Band Transitions for OCS Calibrated Against the 10^00–00^00 Frequencies

11^1e0–01^1e0			11^1f0–01^1f0			20^00–10^00		
Rotational transition	Obs. freq. (unc.)[a] (MHz)	O–C[b] (MHz)	Rotational transition	Obs. freq. (unc.)[a] (MHz)	O–C[b] (MHz)	Rotational transition	Obs. freq. (unc.)[a] (MHz)	O–C[b] (MHz)
$P(41)$	25 016 835 (18)	5	$P(41)$	25 017 087 (18)	−10	$P(41)$	25 015 363 (12)	−15
$P(33)$	25 123 957 (24)	2	$P(33)$	25 124 041 (24)	−7	$P(33)$	25 123 049 (32)	−8
$P(31)$	25 150 399 (34)	−8	$P(31)$	25 150 435 (34)	−29	$P(31)$	25 149 580 (41)	−34
$P(14)$	25 369 904 (12)	8	$P(8)$	25 444 996 (72)	−1	$P(15)$	25 356 839 (12)	6
$P(8)$	25 445 056 (72)	−15	$P(7)$	25 457 428 (50)	13	$P(14)$	25 369 499 (30)	24
$P(7)$	25 457 473 (50)	−10	$P(5)$[c]	25 482 167 (56)	13	$P(8)$	25 444 543 (68)	−10
$P(5)$[c]	25 482 221 (56)	13	$R(1)$[c]	25 567 748 (50)	32	$P(7)$	25 456 940 (50)	3
$R(1)$[c]	25 567 720 (50)	33	$R(4)$	25 603 886 (20)	−9	$P(6)$	25 469 294 (58)	9
$R(4)$	25 603 835 (20)	19	$R(17)$	25 757 254 (50)	12	$P(5)$	25 481 612 (52)	16
$R(17)$	25 756 864 (50)	18	$R(18)$	25 768 802 (40)	−4	$R(1)$	25 566 772 (20)	30
$R(18)$	25 768 376 (40)	−2	$R(19)$	25 780 332 (40)	−4	$R(3)$	25 590 728 (12)	−8
$R(19)$	25 779 882 (40)	6	$R(20)$	25 791 832 (36)	−1	$R(17)$	25 754 538 (72)	14
$R(20)$	25 791 337 (32)	−3	$R(21)$	25 803 299 (32)	3	$R(18)$	25 765 927 (20)	−15
$R(21)$	25 802 774 (28)	5	$R(24)$	25 837 502 (20)	19	$R(19)$	25 777 313 (16)	−10
$R(27)$	25 870 620 (12)	5	$R(27)$	25 871 367 (12)	1	$R(20)$	25 788 678 (12)	13
$R(28)$	25 881 796 (12)	−5	$R(37)$	25 982 092 (40)	0	$R(21)$	25 799 968 (12)	−2
$R(37)$	25 980 890 (48)	−7	$R(43)$	26 046 877 (64)	6	$R(22)$	25 811 240 (20)	3
$R(45)$	26 066 567 (12)	−4	$R(44)$	26 057 532 (64)	−13	$R(24)$	25 833 656 (12)	−1
$R(46)$	26 077 132 (20)	13	$R(45)$	26 068 174 (20)	−10	$R(28)$	25 878 044 (60)	3
$R(47)$	26 087 634 (20)	3	$R(46)$	26 078 790 (16)	2	$R(38)$	25 986 322 (12)	3
$R(62)$	26 240 939 (72)	9	$R(62)$	26 243 601 (50)	10	$R(44)$	26 049 428 (40)	−1
$R(63)$	26 250 847 (12)	−7	$R(63)$	26 253 584 (28)	1	$R(45)$	26 059 810 (48)	−1
$R(64)$	26 260 731 (20)	−10	$R(64)$	26 263 537 (20)	−2	$R(46)$	26 070 147 (36)	−6
$R(65)$	26 270 567 (20)	−24	$R(65)$	26 273 460 (20)	3	$R(47)$	26 080 469 (28)	12
$R(66)$	26 280 400 (35)	−3	$R(66)$	26 283 345 (35)	7	$R(63)$	26 239 922 (80)	7
$R(67)$	26 290 177 (12)	0	$R(68)$	26 303 002 (12)	12	$R(65)$	26 259 124 (30)	−2
$R(68)$	26 299 914 (20)	1	$R(69)$	26 312 748 (12)	−11	$R(66)$	26 268 673 (16)	3
$R(69)$	26 309 618 (22)	6				$R(67)$	26 278 161 (50)	−13
						$R(68)$	26 287 652 (32)	16
						$R(69)$	26 297 051 (40)	−8
						$R(70)$	26 306 443 (48)	3

[a] The estimated uncertainty (primarily associated with temperature instability in the etalon which we believe is the major source of error in these experiments) is given in parentheses in megahertz.

[b] Observed frequencies minus frequencies calculated with the constants given in Table III.

[c] The separation of the e and f components for $P(5)$ and $R(1)$ was estimated, and the unresolved measurements were corrected for this splitting.

Table III. Wave Numbers, Frequencies, and Intensities (at 296 K) of Spectral Lines of the 10^00-00^00 Band of OCS from 815 to 892 cm^{-1}

Wave number (cm^{-1})	Frequency (MHz)	Transition	Intensity (m^{-2} $daPa^{-1}$) or (cm^{-2} atm^{-1})[a]	Wave number (cm^{-1})	Frequency (MHz)	Transition	Intensity (m^{-2} $daPa^{-1}$) or (cm^{-2} atm^{-1})[a]
815.09994(40)	24436081.4(119)	$P(95)$	0.00031	848.02784(4)	25423235.1(12)	$P(26)$	0.34621
815.61764(36)	24451601.6(107)	$P(94)$	0.00037	848.46352(4)	25436296.4(12)	$P(25)$	0.35059
816.13413(32)	24467085.8(96)	$P(93)$	0.00044	848.89801(4)	25449322.0(12)	$P(24)$	0.35377
816.64943(29)	24482534.0(86)	$P(92)$	0.00052	849.33130(4)	25462311.9(12)	$P(23)$	0.35565
817.16353(26)	24497946.3(77)	$P(91)$	0.00061	849.76341(4)	25475266.0(12)	$P(22)$	0.35616
817.67643(23)	24513322.7(68)	$P(90)$	0.00073	850.19432(4)	25488184.5(12)	$P(21)$	0.35524
818.18813(20)	24528663.1(61)	$P(89)$	0.00086	850.62404(4)	25501067.2(12)	$P(20)$	0.35282
818.69864(18)	24543967.7(54)	$P(88)$	0.00101	851.05257(4)	25513914.1(12)	$P(19)$	0.34884
819.20794(16)	24559236.3(48)	$P(87)$	0.00119	851.47990(4)	25526725.2(12)	$P(18)$	0.34328
819.71606(14)	24574469.2(42)	$P(86)$	0.00140	851.90604(4)	25539500.5(12)	$P(17)$	0.33611
820.22297(12)	24589666.2(37)	$P(85)$	0.00163	852.33098(4)	25552240.0(13)	$P(16)$	0.32729
820.72870(11)	24604827.3(33)	$P(84)$	0.00191	852.75473(4)	25564943.6(13)	$P(15)$	0.31684
821.23322(10)	24619952.7(30)	$P(83)$	0.00223	853.17728(4)	25577611.4(13)	$P(14)$	0.30476
821.73656(9)	24635042.3(27)	$P(82)$	0.00259	853.59863(4)	25590243.2(13)	$P(13)$	0.29106
822.23870(8)	24650096.1(24)	$P(81)$	0.00301	854.01879(4)	25602839.2(13)	$P(12)$	0.27579
822.73965(7)	24665114.1(22)	$P(80)$	0.00349	854.43775(4)	25615399.2(13)	$P(11)$	0.25900
823.23940(7)	24680096.4(21)	$P(79)$	0.00404	854.85550(4)	25627923.3(13)	$P(10)$	0.24074
823.7379(7)	24695043.0(20)	$P(78)$	0.00466	855.27206(4)	25640411.4(13)	$P(9)$	0.22110
824.23534(7)	24709953.9(20)	$P(77)$	0.00536	855.68742(4)	25652863.4(13)	$P(8)$	0.20016
824.73152(6)	24724829.0(19)	$P(76)$	0.00616	856.10157(4)	25665279.4(13)	$P(7)$	0.17801
825.22651(6)	24739668.5(19)	$P(75)$	0.00707	856.51452(4)	25677659.4(13)	$P(6)$	0.15478
825.72032(6)	24754472.3(19)	$P(74)$	0.00809	856.92627(4)	25690003.3(13)	$P(5)$	0.13059
826.21293(6)	24769240.5(19)	$P(73)$	0.00924	857.33681(4)	25702311.0(13)	$P(4)$	0.10556
826.70435(6)	24783973.0(19)	$P(72)$	0.01052	857.74615(4)	25714582.6(13)	$P(3)$	0.07984
827.19459(6)	24798669.8(19)	$P(71)$	0.01196	858.15428(4)	25726818.0(13)	$P(2)$	0.05357
827.68363(6)	24813331.1(19)	$P(70)$	0.01357	858.56120(4)	25739017.3(13)	$P(1)$	0.02690
828.17149(6)	24827956.7(19)	$P(69)$	0.01536	859.37142(4)	25763306.9(13)	$R(0)$	0.02698
828.65816(6)	24842546.7(19)	$P(68)$	0.01735	859.77471(4)	25775397.4(13)	$R(1)$	0.05389
829.14364(6)	24857101.1(19)	$P(67)$	0.01956	860.17679(4)	25787451.4(13)	$R(2)$	0.08055
829.62794(6)	24871619.9(19)	$P(66)$	0.02200	860.57766(4)	25799469.1(13)	$R(3)$	0.10682
830.11105(6)	24886103.2(19)	$P(65)$	0.02469	860.97731(4)	25811450.5(13)	$R(4)$	0.13255
830.59297(6)	24900550.9(18)	$P(64)$	0.02764	861.37575(4)	25823395.3(13)	$R(5)$	0.15757
831.07371(6)	24914963.0(18)	$P(63)$	0.03088	861.77297(4)	25835303.7(13)	$R(6)$	0.18176
831.55326(6)	24929339.5(17)	$P(62)$	0.03443	862.16898(4)	25847175.6(13)	$R(7)$	0.20498
832.03162(6)	24943680.6(17)	$P(61)$	0.03829	862.56376(4)	25859011.0(13)	$R(8)$	0.22710
832.50880(6)	24957986.0(17)	$P(60)$	0.04250	862.95733(4)	25870809.8(13)	$R(9)$	0.24802
832.98480(5)	24972256.0(16)	$P(59)$	0.04706	863.34967(4)	25882571.9(13)	$R(10)$	0.26762
833.45961(5)	24986490.4(16)	$P(58)$	0.05199	863.74079(4)	25894297.4(13)	$R(11)$	0.28582
833.93323(5)	25000689.3(15)	$P(57)$	0.05731	864.13069(4)	25905986.2(13)	$R(12)$	0.30255
834.40567(5)	25014852.7(15)	$P(56)$	0.06304	864.51936(4)	25917638.3(13)	$R(13)$	0.31773
834.87692(5)	25028980.5(14)	$P(55)$	0.06917	864.90680(4)	25929253.6(13)	$R(14)$	0.33131
835.34699(5)	25043072.9(14)	$P(54)$	0.07573	865.29302(4)	25940832.1(12)	$R(15)$	0.34326
835.81588(4)	25057129.7(13)	$P(53)$	0.08272	865.67801(4)	25952373.7(12)	$R(16)$	0.35355
836.28358(4)	25071151.0(13)	$P(52)$	0.09014	866.06176(4)	25963878.4(12)	$R(17)$	0.36218
836.75010(4)	25085136.8(13)	$P(51)$	0.09800	866.44428(4)	25975346.2(12)	$R(18)$	0.36914
837.21543(4)	25099087.1(12)	$P(50)$	0.10630	866.82557(4)	25986777.0(12)	$R(19)$	0.37446
837.67958(4)	25113001.9(12)	$P(49)$	0.11503	867.20563(4)	25998170.7(12)	$R(20)$	0.37815
838.14254(4)	25126881.2(12)	$P(48)$	0.12417	867.58445(4)	26009527.4(12)	$R(21)$	0.38027
838.60432(4)	25140725.0(12)	$P(47)$	0.13372	867.96203(4)	26020846.9(12)	$R(22)$	0.38085
839.06491(4)	25154533.3(11)	$P(46)$	0.14366	868.33837(4)	26032129.3(12)	$R(23)$	0.37997
839.52432(4)	25168306.1(11)	$P(45)$	0.15396	868.71346(4)	26043374.5(12)	$R(24)$	0.37768
839.98255(4)	25182043.3(11)	$P(44)$	0.16459	869.08732(4)	26054582.3(12)	$R(25)$	0.37407
840.43959(4)	25195745.1(11)	$P(43)$	0.17552	869.45993(4)	26065752.9(12)	$R(26)$	0.36921
840.89545(4)	25209411.3(11)	$P(42)$	0.18671	869.83129(4)	26076886.1(12)	$R(27)$	0.36320
841.35012(4)	25223042.0(11)	$P(41)$	0.19811	870.20141(4)	26087981.9(12)	$R(28)$	0.35613
841.80360(4)	25236637.2(11)	$P(40)$	0.20966	870.57027(4)	26099040.3(12)	$R(29)$	0.34810
842.25591(4)	25250196.8(11)	$P(39)$	0.22131	870.93789(4)	26110061.1(12)	$R(30)$	0.33920
842.70702(4)	25263720.9(11)	$P(38)$	0.23300	871.30425(4)	26121044.3(12)	$R(31)$	0.32953
843.15695(4)	25277209.5(11)	$P(37)$	0.24465	871.66936(4)	26131990.0(12)	$R(32)$	0.31919
843.60569(4)	25290662.5(11)	$P(36)$	0.25619	872.03321(4)	26142897.9(12)	$R(33)$	0.30829
844.05325(4)	25304079.9(12)	$P(35)$	0.26754	872.39580(4)	26153768.2(11)	$R(34)$	0.29692
844.49962(4)	25317461.8(12)	$P(34)$	0.27862	872.75713(4)	26164600.6(11)	$R(35)$	0.28517
844.94481(4)	25330808.1(12)	$P(33)$	0.28933	873.11720(4)	26175395.2(11)	$R(36)$	0.27313
845.38881(4)	25344118.8(12)	$P(32)$	0.29959	873.47601(4)	26186152.0(11)	$R(37)$	0.26090
845.83162(4)	25357393.9(12)	$P(31)$	0.30930	873.83355(4)	26196870.8(11)	$R(38)$	0.24855
846.27324(4)	25370633.4(12)	$P(30)$	0.31836	874.18982(4)	26207551.6(11)	$R(39)$	0.23617
846.71367(4)	25383837.3(12)	$P(29)$	0.32668	874.54483(4)	26218194.3(11)	$R(40)$	0.22382
847.15292(4)	25397005.6(12)	$P(28)$	0.33416				
847.59097(4)	25410138.2(12)	$P(27)$	0.34070				

continued

Table III, continued

Wave number (cm^{-1})	Frequency (MHz)	Transition	Intensity (m^{-2} daPa^{-1}) or (cm^{-2} atm^{-1})[a]
874.89856(4)	26228798.9(11)	R(41)	0.21157
875.25102(4)	26239365.4(11)	R(42)	0.19949
875.60220(4)	26249893.6(11)	R(43)	0.18762
875.95211(4)	26260383.5(11)	R(44)	0.17602
876.30073(4)	26270835.0(12)	R(45)	0.16474
876.64808(4)	26281248.2(12)	R(46)	0.15380
876.99414(4)	26291622.9(12)	R(47)	0.14324
877.33892(4)	26301959.0(12)	R(48)	0.13308
877.68240(4)	26312256.5(13)	R(49)	0.12335
878.02460(4)	26322515.4(13)	R(50)	0.11407
878.36551(4)	26332735.6(13)	R(51)	0.10523
878.70512(5)	26342916.9(14)	R(52)	0.09685
879.04344(5)	26353059.4(14)	R(53)	0.08893
879.38046(5)	26363163.0(15)	R(54)	0.08147
879.71618(5)	26373227.6(15)	R(55)	0.07447
880.05060(5)	26383253.2(16)	R(56)	0.06791
880.38371(5)	26393239.6(16)	R(57)	0.06179
880.71551(6)	26403186.8(17)	R(58)	0.05609
881.04601(6)	26413094.8(17)	R(59)	0.05081
881.37519(6)	26422963.5(17)	R(60)	0.04591
881.70306(6)	26432792.8(18)	R(61)	0.04140
882.02961(6)	26442582.6(18)	R(62)	0.03725
882.35485(6)	26452332.9(19)	R(63)	0.03344
882.67876(6)	26462043.6(19)	R(64)	0.02995
883.00135(6)	26471714.6(19)	R(65)	0.02677
883.32262(6)	26481345.9(19)	R(66)	0.02388
883.64255(6)	26490937.3(19)	R(67)	0.02125
883.96116(6)	26500488.9(19)	R(68)	0.01887
884.27843(6)	26510000.5(19)	R(69)	0.01671
884.59437(6)	26519472.1(19)	R(70)	0.01478
884.90897(6)	26528903.6(19)	R(71)	0.01304
885.22223(6)	26538294.9(19)	R(72)	0.01148
885.53415(6)	26547646.0(19)	R(73)	0.01008
885.84472(6)	26556956.7(19)	R(74)	0.00884
886.15395(7)	26566227.0(20)	R(75)	0.00773
886.46182(7)	26575456.8(20)	R(76)	0.00674
886.76834(7)	26584646.1(21)	R(77)	0.00587
887.07351(7)	26593794.8(22)	R(78)	0.00511
887.37732(8)	26602902.7(24)	R(79)	0.00443
887.67976(9)	26611969.8(27)	R(80)	0.00383
887.98085(10)	26620996.1(29)	R(81)	0.00331
888.28057(11)	26629981.5(33)	R(82)	0.00285
888.57892(12)	26638925.8(37)	R(83)	0.00245
888.87590(14)	26647829.0(42)	R(84)	0.00210
889.17150(16)	26656691.0(48)	R(85)	0.00180
889.46573(18)	26665511.8(54)	R(86)	0.00154
889.75858(20)	26674291.2(61)	R(87)	0.00131
890.05005(23)	26683029.2(68)	R(88)	0.00112
890.34013(26)	26691725.7(77)	R(89)	0.00095
890.62883(29)	26700380.7(86)	R(90)	0.00080
890.91614(32)	26708993.9(96)	R(91)	0.00068
891.20205(36)	26717565.5(107)	R(92)	0.00057
891.48657(40)	26726095.1(119)	R(93)	0.00048
891.76970(44)	26734582.9(131)	R(94)	0.00041
892.05142(48)	26743028.7(145)	R(95)	0.00034

[a] To within the accuracy of the intensity data, 1 m^{-2} daPa^{-1} is equal to 1 cm^{-2} atm^{-1}.

Since the data span the range of rotational quantum numbers from $J = 0$ to $J = 88$, the H term was tentatively included in Eq. (1). In agreement with earlier conclusions,[10] it was found that the ground state data could be fit quite well with $H_0 = 0$. On the other hand, the data were fit somewhat better when H was included as a variable for the fits involving the 20^00 and 10^00 states. Even though the uncertainty in the H term is very large, it was included in the analysis of transitions involving those states.

Since one goal of this work was to obtain data for the calculation of the 20^00–00^00 transitions near 1700 cm^{-1}, the 10^00–00^00 and 20^00–10^00 transitions were analyzed together. This analysis yielded the variance–covariance matrix elements needed to calculate the uncertainties for the calculated 20^00–00^00 transitions.

The constants given in Table IV and the variance–covariance matrix elements were used to calculate the frequency calibration data given as Tables III and V. In these tables, the calculated uncertainty in each transition frequency is given in parentheses following each entry. This uncertainty is twice the estimated standard deviation obtained from the statistical analysis. This extra factor of 2 was used somewhat arbitrarily to give what we believe is a better estimate of the absolute uncertainty since the statistically determined uncertainty is always less than the absolute uncertainty in the frequency because of systematic errors.

One possible source of systematic error could be due to a pressure shifting of the OCS absorption lines. The magnitude of the pressure shift is probably about a tenth of the pressure broadening effect which is <75 kHz/Pa (10 MHz/Torr). Since the measurements on the 10^00–00^00 band were made with OCS pressures smaller than 66 Pa (0.5 Torr), the pressure shift is expected to be <0.5 MHz. Since the 20^00–10^00 band measurements were made at pressures as high as 266 Pa (2 Torr), frequency shifts as large as 2 MHz might affect those measurements. However, since the weaker high J transitions are the ones most likely to have smaller pressure shifts, we expect that the errors due to pressure shifts will be smaller than the standard deviations given by the random errors in the measurements. Unfortunately, we are unable to quantify more precisely the sources of systematic error which might affect our results.

The reader is cautioned not to use the constants given in Table IV to calculate transitions beyond the $J = 95$ cutoff that was used for making Tables III and V. Such extrapolations beyond the range of measured transitions are unreliable.

In the analysis of the data for the $l = 1$ vibrational transition (11^10–01^10), the following term value equations were used:

$$T(v,J) = F(v) + B_vJ(J+1) \pm 0.5q_vJ(J+1) - D_v[J(J+1)-1]^2 \mp 0.5q_{vJ}J^2(J+1)^2, \quad (3)$$

$$\nu_0(v' \leftarrow v'') = F(v') - F(v''). \quad (4)$$

Table IV. Constants [a] for OCS Determined from These Measurements

Constant	This work (MHz) [b]	Previous work (Ref. 4) (MHz)
ν_0 (20^00–00^00)	51 293 779.3 (19)	51 293 779. (111)
ν_0 (10^00–00^00)	25 751 180.2 (6)	25 751 204. (65)
ν_0 (20^00–10^00)	25 542 599.0 (18)	—
ν_0 (11^10–01^10)	25 543 432.7 (14)	25 543 403. (75)
B (00^00)	6081.492518 (56)	(6081.4924439) [c]
D (00^00)	1.3019369 (114) × 10^{-3}	(1.301789 × 10^{-3}) [c]
B (10^00)	6063.358265 (200)	6063.3588 (8)
D (10^00)	1.329873 (197) × 10^{-3}	1.3312 (19) × 10^{-3}
H (10^00)	0.0001214 (276) × 10^{-6}	—
B (20^00)	6044.874923 (2550)	6044.891 (5)
D (20^00))	1.359731 (810) × 10^{-3}	1.3607 (10) × 10^{-3}
H (20^00)	0.0002234 (706) × 10^{-6}	—
B (01^10)	6092.078222 (289)	—
D (01^10)	1.323567 (625) × 10^{-3}	—
q (01^10)	6.361411394 (745)	—
q_J (01^10)	4.25608 (667) × 10^{-6}	—
B (11^10)	6075.50528 (186)	6075.519 (7)
D (11^10)	1.362242 (6q (11^10)	6.853553 (2121)
6.853 (13)		
q_J (11^10)	11.670 (489) × 10^{-6}	—

[a] The statistically estimated uncertainties in the last digits (one standard deviation) are given in parentheses following each value. Since systematic errors have not been taken into account, these estimated uncertainties may be slightly optimistic.

[b] To convert from frequency units to wave number units, use 299 792 458 m/sec for the speed of light.[16]

[c] See Ref. 10; the negligible difference in the B_0 and D_0 values given in Ref. 10 and in this work arises from the inclusion of an H_0 term in Ref. 10.

For both the 11^10 and 01^10 states, the upper sign in Eq. (3) applies for the f rotational levels and the lower sign applies for the e rotational levels. As before, the data given in Tables I and II were combined with appropriate microwave transitions[10,11] in a weighted least squares fit. Insufficient data were available to warrant extending Eq. (3) to include the higher order H term.

IV. Description and Analysis of the Intensity Data

Preliminary intensity measurements have been made on several lines of the 10^00–00^00 band using the technique of measuring the intensity at the line center, as was done on the $2\nu_2$ band[1] and as advocated by Jennings.[12] Contrary to our initial expectation, such intensity measurements are not entirely free of instrumental resolution problems.

It was found that some of the measurements implied intensities that were clearly too low. When heterodyne measurements of the frequency width of the diode laser output were possible, it was found that the low intensity measurements were due to large laser linewidths. Since the Doppler halfwidth of the OCS lines is only ~20 MHz, accurate intensity measurements of the absorption peak are only possible if the laser linewidth is <3 MHz. Should the laser linewidth be >3 MHz, the measured peak intensity would be smaller than the true intensity. Our limited experience has indicated that most diode lasers will give unacceptably large output linewidths at certain frequencies although the same diode may have very narrow linewidths at other frequencies. The best way to ensure that this instrumental problem is not affecting the measurements is to measure simultaneously the diode laser linewidth by beating it against a narrow line gas laser, such as a CO_2 laser.

The most reliable intensity measurements were made on the $R(28)$ and $R(33)$ lines of the 10^00–00^00 band. Measurements were made using a 50-cm absorption cell and pressure of the order of 12 Pa (0.09 Torr). The signal representing 100% absorption was determined by blocking the laser beam with an opaque shutter. The absence of stray radiation was verified by observing that the opaque shutter gave the same signal level as was given by saturated absorption lines when the cell was filled to a pressure of 50 Torr of OCS.

At 296 K, the line intensity for $R(28)$ was found to be ~3.4 cm^{-2} MPa^{-1} (0.34 cm^{-2} atm^{-1}) and for $R(33)$ it was ~3.1 cm^{-2} MPa^{-1} (0.31 cm^{-2} atm^{-1}) with an uncertainty of ~10%. This gives a transition moment of 0.0632 D and an integrated intensity of ~350 cm^{-2} MPa^{-1} (35 cm^{-2} atm^{-1}) for all isotopes and hot bands in the ν_1 region. This value is close to 340 cm^{-2} MPa^{-1} (34 cm^{-2} atm^{-1}) given by Robinson,[13] and the transition moment of 0.0632 D is close to the value of 0.0681 D given by Foord and Whiffen.[14] Tables III and V give estimated line intensities in units of cm^{-2} atm^{-1} calculated for a temperature of 296 K. To convert the latter intensity units to the frequently used spectroscopic units of cm/molecule, one should divide by 2.479 × 10^{19} molecules · cm^{-3} · atm^{-1}.

Table V. Wave Numbers, Frequencies, and Intensities (at 296 K) of Spectral Lines of the 20^00-00^00 Band of OCS from 1662 to 1738 cm^{-1}

Wave number (cm^{-1})	Frequency (MHz)	Transition	Intensity (m^{-2} $daPa^{-1}$) or (cm^{-2} atm^{-1})[a]
1661.52665(49)	49811315.8(148)	$P(95)$	0.00005
1662.16342(43)	49830405.6(130)	$P(94)$	0.00006
1662.79765(38)	49849419.5(114)	$P(93)$	0.00008
1663.42936(33)	49868357.6(99)	$P(92)$	0.00009
1664.05854(29)	49887220.0(86)	$P(91)$	0.00011
1664.68520(25)	49906006.8(75)	$P(90)$	0.00013
1665.30934(22)	49924718.1(66)	$P(89)$	0.00015
1665.93096(19)	49943353.9(57)	$P(88)$	0.00018
1666.55007(17)	49961914.3(51)	$P(87)$	0.00021
1667.16667(15)	49980399.3(46)	$P(86)$	0.00024
1667.78075(14)	49998809.1(42)	$P(85)$	0.00028
1668.39233(13)	50017143.7(40)	$P(84)$	0.00033
1669.00140(13)	50035403.2(38)	$P(83)$	0.00039
1669.60797(12)	50053587.6(37)	$P(82)$	0.00045
1670.21203(12)	50071697.1(37)	$P(81)$	0.00052
1670.81360(12)	50089731.6(37)	$P(80)$	0.00061
1671.41267(12)	50107691.3(37)	$P(79)$	0.00070
1672.00925(12)	50125576.1(37)	$P(78)$	0.00081
1672.60333(12)	50143386.3(37)	$P(77)$	0.00093
1673.19492(12)	50161121.8(37)	$P(76)$	0.00107
1673.78403(12)	50178782.7(37)	$P(75)$	0.00122
1674.37064(12)	50196369.1(37)	$P(74)$	0.00140
1674.95478(12)	50213881.0(37)	$P(73)$	0.00160
1675.53643(12)	50231318.5(37)	$P(72)$	0.00182
1676.11560(12)	50248681.6(37)	$P(71)$	0.00207
1676.69230(12)	50265970.5(36)	$P(70)$	0.00235
1677.26651(12)	50283185.1(36)	$P(69)$	0.00266
1677.83826(12)	50300325.5(35)	$P(68)$	0.00300
1678.40753(12)	50317391.8(35)	$P(67)$	0.00338
1678.97432(11)	50334384.0(34)	$P(66)$	0.00380
1679.53865(11)	50351302.1(34)	$P(65)$	0.00426
1680.10052(11)	50368146.3(33)	$P(64)$	0.00477
1680.65991(11)	50384916.6(33)	$P(63)$	0.00533
1681.21684(11)	50401613.0(33)	$P(62)$	0.00594
1681.77131(11)	50418235.6(32)	$P(61)$	0.00660
1682.32332(11)	50434784.4(32)	$P(60)$	0.00733
1682.87287(11)	50451259.5(32)	$P(59)$	0.00811
1683.41996(11)	50467660.9(32)	$P(58)$	0.00896
1683.96460(11)	50483988.6(32)	$P(57)$	0.00987
1684.50678(11)	50500242.7(32)	$P(56)$	0.01085
1685.04650(11)	50516423.3(32)	$P(55)$	0.01191
1685.58378(11)	50532530.4(32)	$P(54)$	0.01303
1686.11860(11)	50548564.0(32)	$P(53)$	0.01423
1686.65097(10)	50564524.1(31)	$P(52)$	0.01550
1687.18090(10)	50580410.9(31)	$P(51)$	0.01685
1687.70838(10)	50596224.2(31)	$P(50)$	0.01827
1688.23341(10)	50611964.3(31)	$P(49)$	0.01977
1688.75599(10)	50627631.0(31)	$P(48)$	0.02133
1689.27614(10)	50643224.5(31)	$P(47)$	0.02297
1689.79384(10)	50658744.8(30)	$P(46)$	0.02467
1690.30909(10)	50674191.8(30)	$P(45)$	0.02643
1690.82191(10)	50689565.7(30)	$P(44)$	0.02825
1691.33229(10)	50704866.4(29)	$P(43)$	0.03011
1691.84023(10)	50720094.0(29)	$P(42)$	0.03202
1692.34573(10)	50735248.5(29)	$P(41)$	0.03397
1692.84879(9)	50750329.9(28)	$P(40)$	0.03594
1693.34941(9)	50765338.3(28)	$P(39)$	0.03793
1693.84760(9)	50780273.6(27)	$P(38)$	0.03992
1694.34336(9)	50795136.0(27)	$P(37)$	0.04190
1694.83668(9)	50809925.3(26)	$P(36)$	0.04387
1695.32756(9)	50824641.7(26)	$P(35)$	0.04580
1695.81601(8)	50839285.1(25)	$P(34)$	0.04768
1696.30203(8)	50853855.5(25)	$P(33)$	0.04950
1696.78562(8)	50868353.1(25)	$P(32)$	0.05124
1697.26677(8)	50882777.7(24)	$P(31)$	0.05289
1697.74549(8)	50897129.4(24)	$P(30)$	0.05442
1698.22178(8)	50911408.2(24)	$P(29)$	0.05583
1698.69564(8)	50925614.2(24)	$P(28)$	0.05709
1699.16707(8)	50939747.2(24)	$P(27)$	0.05820
1699.63607(8)	50953807.4(24)	$P(26)$	0.05912
1700.10263(8)	50967794.7(25)	$P(25)$	0.05985
1700.56677(8)	50981709.1(25)	$P(24)$	0.06038
1701.02847(9)	50995550.7(26)	$P(23)$	0.06068
1701.48775(9)	51009319.4(26)	$P(22)$	0.06075
1701.94459(9)	51023015.2(27)	$P(21)$	0.06058
1702.39900(9)	51036638.2(28)	$P(20)$	0.06015
1702.85099(9)	51050188.3(28)	$P(19)$	0.05946
1703.30054(10)	51063665.5(29)	$P(18)$	0.05849
1703.74766(10)	51077069.8(30)	$P(17)$	0.05725
1704.19235(10)	51090401.3(31)	$P(16)$	0.05574
1704.63460(11)	51103659.8(32)	$P(15)$	0.05394
1705.07443(11)	51116845.4(32)	$P(14)$	0.05187
1705.51182(11)	51129958.1(33)	$P(13)$	0.04953
1705.94678(11)	51142997.9(34)	$P(12)$	0.04692
1706.37931(12)	51155964.7(35)	$P(11)$	0.04405
1706.80940(12)	51168858.6(35)	$P(10)$	0.04093
1707.23706(12)	51181679.4(36)	$P(9)$	0.03758
1707.66228(12)	51194427.3(36)	$P(8)$	0.03401
1708.08507(12)	51207102.1(37)	$P(7)$	0.03024
1708.50542(12)	51219703.9(37)	$P(6)$	0.02629
1708.92333(13)	51232232.6(38)	$P(5)$	0.02217
1709.33881(13)	51244688.2(38)	$P(4)$	0.01792
1709.75184(13)	51257070.7(38)	$P(3)$	0.01355
1710.16244(13)	51269380.1(38)	$P(2)$	0.00909
1710.57059(13)	51281616.3(39)	$P(1)$	0.00456
1711.37958(13)	51305869.0(38)	$R(0)$	0.00457
1711.78040(13)	51317885.5(38)	$R(1)$	0.00913
1712.17879(13)	51329828.7(38)	$R(2)$	0.01365
1712.57472(13)	51341698.5(38)	$R(3)$	0.01810
1712.96821(12)	51353495.0(37)	$R(4)$	0.02245
1713.35925(12)	51365218.0(37)	$R(5)$	0.02668
1713.74784(12)	51376867.6(36)	$R(6)$	0.03076
1714.13397(12)	51388443.7(36)	$R(7)$	0.03469
1714.51766(12)	51399946.3(35)	$R(8)$	0.03842
1714.89889(12)	51411375.3(35)	$R(9)$	0.04195
1715.27766(11)	51422730.6(34)	$R(10)$	0.04525
1715.65398(11)	51434012.3(33)	$R(11)$	0.04831
1716.02784(11)	51445220.3(32)	$R(12)$	0.05113
1716.39923(11)	51456354.5(32)	$R(13)$	0.05368
1716.76817(10)	51467414.9(31)	$R(14)$	0.05596
1717.13464(10)	51478401.4(30)	$R(15)$	0.05796
1717.49864(10)	51489314.0(29)	$R(16)$	0.05969
1717.86018(9)	51500152.7(28)	$R(17)$	0.06113
1718.21925(9)	51510917.2(28)	$R(18)$	0.06228
1718.57585(9)	51521607.7(27)	$R(19)$	0.06317
1718.92997(9)	51532224.1(26)	$R(20)$	0.06377
1719.28162(9)	51542766.2(26)	$R(21)$	0.06411
1719.63079(8)	51553234.1(25)	$R(22)$	0.06419
1719.97748(8)	51563627.6(25)	$R(23)$	0.06403
1720.32169(8)	51573946.7(24)	$R(24)$	0.06363
1720.66341(8)	51584191.4(24)	$R(25)$	0.06300
1721.00265(8)	51594361.5(24)	$R(26)$	0.06217
1721.33940(8)	51604457.0(24)	$R(27)$	0.06114
1721.67366(8)	51614477.9(24)	$R(28)$	0.05993
1722.00543(8)	51624424.0(24)	$R(29)$	0.05857
1722.33470(8)	51634295.3(24)	$R(30)$	0.05705
1722.66147(8)	51644091.8(25)	$R(31)$	0.05541
1722.98575(8)	51653813.2(25)	$R(32)$	0.05366
1723.30752(9)	51663459.7(26)	$R(33)$	0.05182
1723.62678(9)	51673031.0(26)	$R(34)$	0.04989
1723.94354(9)	51682527.1(27)	$R(35)$	0.04791
1724.25778(9)	51691948.0(27)	$R(36)$	0.04587
1724.56952(9)	51701293.4(28)	$R(37)$	0.04381
1724.87873(9)	51710563.5(28)	$R(38)$	0.04172
1725.18543(10)	51719758.1(29)	$R(39)$	0.03963
1725.48960(10)	51728877.0(29)	$R(40)$	0.03755
1725.79126(10)	51737920.2(29)	$R(41)$	0.03549

continued

Table V, continued

Wave number (cm^{-1})	Frequency (MHz)	Transition	Intensity (m^{-2} daPa^{-1}) or (cm^{-2} atm^{-1})[a]
1726.09038(10)	51746887.7(30)	$R(42)$	0.03345
1726.38697(10)	51755779.3(30)	$R(43)$	0.03145
1726.68103(10)	51764594.9(30)	$R(44)$	0.02950
1726.97255(10)	51773334.5(31)	$R(45)$	0.02760
1727.26153(10)	51781998.0(31)	$R(46)$	0.02576
1727.54797(10)	51790585.2(31)	$R(47)$	0.02399
1727.83186(10)	51799096.1(31)	$R(48)$	0.02228
1728.11321(10)	51807530.6(31)	$R(49)$	0.02065
1728.39200(10)	51815888.5(31)	$R(50)$	0.01909
1728.66823(11)	51824169.8(32)	$R(51)$	0.01761
1728.94191(11)	51832374.4(32)	$R(52)$	0.01620
1729.21302(11)	51840502.2(32)	$R(53)$	0.01487
1729.48157(11)	51848553.1(32)	$R(54)$	0.01362
1729.74755(11)	51856526.9(32)	$R(55)$	0.01245
1730.01095(11)	51864423.6(32)	$R(56)$	0.01135
1730.27178(11)	51872243.1(32)	$R(57)$	0.01032
1730.53003(11)	51879985.2(32)	$R(58)$	0.00937
1730.78570(11)	51887649.9(32)	$R(59)$	0.00848
1731.03878(11)	51895237.0(33)	$R(60)$	0.00766
1731.28926(11)	51902746.4(33)	$R(61)$	0.00691
1731.53716(11)	51910178.1(33)	$R(62)$	0.00622
1731.78245(11)	51917531.8(34)	$R(63)$	0.00558
1732.02515(11)	51924807.6(34)	$R(64)$	0.00500
1732.26523(12)	51932005.3(35)	$R(65)$	0.00446
1732.50271(12)	51939124.7(35)	$R(66)$	0.00398
1732.73758(12)	51946165.7(36)	$R(67)$	0.00354
1732.96983(12)	51953128.3(36)	$R(68)$	0.00314
1733.19945(12)	51960012.4(37)	$R(69)$	0.00278
1733.42645(12)	51966817.7(37)	$R(70)$	0.00246
1733.65082(12)	51973544.2(37)	$R(71)$	0.00217
1733.87256(12)	51980191.7(37)	$R(72)$	0.00191
1734.09166(12)	51986760.2(37)	$R(73)$	0.00168
1734.30812(12)	51993249.5(37)	$R(74)$	0.00147
1734.52194(12)	51999659.4(37)	$R(75)$	0.00129
1734.73310(12)	52005990.0(37)	$R(76)$	0.00112
1734.94161(12)	52012240.9(37)	$R(77)$	0.00098
1735.14746(12)	52018412.2(37)	$R(78)$	0.00085
1735.35065(12)	52024503.7(37)	$R(79)$	0.00074
1735.55117(12)	52030515.2(37)	$R(80)$	0.00064
1735.74902(13)	52036446.6(38)	$R(81)$	0.00055
1735.94420(13)	52042297.8(40)	$R(82)$	0.00047
1736.13669(14)	52048068.7(42)	$R(83)$	0.00041
1736.32651(15)	52053759.1(46)	$R(84)$	0.00035
1736.51363(17)	52059368.9(51)	$R(85)$	0.00030
1736.69806(19)	52064898.0(57)	$R(86)$	0.00026
1736.87979(22)	52070346.2(66)	$R(87)$	0.00022
1737.05882(25)	52075713.4(75)	$R(88)$	0.00019
1737.23515(29)	52080999.5(86)	$R(89)$	0.00016
1737.40876(33)	52086204.3(99)	$R(90)$	0.00013
1737.57966(38)	52091327.6(114)	$R(91)$	0.00011
1737.74783(43)	52096369.4(130)	$R(92)$	0.00010
1737.91328(49)	52101329.5(148)	$R(93)$	0.00008
1738.07601(56)	52106207.8(168)	$R(94)$	0.00007
1738.23599(63)	52111004.1(190)	$R(95)$	0.00006

[a] To within the accuracy of the intensity data, 1 m^{-2} daPa^{-1} is equal to 1 cm^{-2} atm^{-1}.

The line intensities for the $2\nu_1$ band given in Table V were based on a value of 61 cm^{-2} MPa^{-1} (6.1 cm^{-2} atm^{-1}) for the integrated total band intensity as recently measured by Kagann.[15] This value is equivalent to a transition moment of 0.0183 D, which is close to 0.021 D measured by Foord and Whiffen.[14]

We have measured frequencies of the OCS spectrum at 11.6 μm using laser frequency metrology techniques which permit better than an order of magnitude improvement in the constants used to calculate the frequencies. These predicted frequencies (for both the 10^00–00–00 and 20^00–00^00 bands) are presented here for immediate use as reference standards. The ultimate goal of this and subsequent heterodyne measurements on the other bands is to facilitate an exact analysis of OCS as a whole in order to provide the best OCS standard frequencies possible.

We wish to express our deep appreciation to Andre Fayt of the University of Louvain, Louvain-la-Neuve, Belgium, for providing us some of his calculations on OCS line positions. We are also grateful to the NASA Upper Atmosphere Research Office for partial support of this program.

References

1. J. S. Wells, F. R. Petersen, and A. G. Maki, Appl. Opt. **18,** 3567 (1979).
2. F. R. Petersen, D. G. McDonald, J. D. Capp, and B. L. Danielson, in *Laser Spectroscopy*, R. G. Brewer and A. Mooradian, Eds. (Plenum, New York, 1974).
3. J. Sattler, Harry Diamond Laboratories, Adelphi, Md.; private communication.
4. A. G. Maki, W. B. Olson, and R. L. Sams, J. Mol. Spectrosc. **81,** 122 (1980).
5. C. Freed and A. Javan, Appl. Phys. Lett. **17,** 53 (1970).
6. C. Freed, A. H. M. Ross, and R. G. O'Donnell, J. Mol. Spectrosc. **49,** 439 (1974).
7. C. Freed, L. C. Bradley, and R. G. O'Donnell, IEEE. J. Quantum Electron **16,** 1195 (1980).
8. F. R. Petersen, J. S. Wells, A. G. Maki, and K. Siemsen, (submitted to Appl. Opt.)
9. A. Fayt, U. Louvain, Louvain-la-Neuve, Belgium; private communication.
10. A. G. Maki, J. Phys. Chem. Ref. Data **3,** 221 (1974).
11. N. W. Larsen and B. P. Winnewisser, Z. Naturforsch Teil A: **29,** 1213 (1974).
12. D. E. Jennings, Appl. Opt. **19,** 2695 (1980).
13. D. Z. Robinson, J. Chem. Phys. **19,** 881 (1951).
14. A. Foord and D. H. Whiffen, Mol. Phys. **26,** 959 (1973).
15. R. Kagann, NBS, Washington, D.C.; private communication.
16. J. Terrien, Metrologia **10,** 9 (1974).

Reprinted from **Applied Optics,** Vol. 20, page 2874, September 1, 1981

Heterodyne frequency measurements on the 11.6-μm band of OCS: new frequency/wavelength calibration tables for 11.6- and 5.8-μm OCS bands: erratum

J. S. Wells, F. R. Petersen, A. G. Maki, and D. J. Sukle

D. J. Sukle is with Community College of Denver, Division of Science, Westminister, Colorado 80030; A. G. Maki is with U.S. National Bureau of Standards, Molecular Spectroscopy Division, Washington, D.C. 20234; the other authors are with U.S. National Bureau of Standards, Time & Frequency Division, Boulder, Colorado 80303.

Received 26 May 1981.

The penultimate line in the body of Table IV of this paper[1] was garbled in the printing process. It is run below correctly.

Table IV. Constant [a] for OCS Determined from These Measurements

Constant	This work (MHz)[b]	Previous work[4] (MHz)
ν_0 (20^00–00^00)	51 293 779.3 (19)	51 293 779. (111)
ν_0 (10^00–00^00)	25 751 180.2 (6)	25 751 204. (65)
ν_0 (20^00–10^00)	25 542 599.0 (18)	—
ν_0 (11^10–01^10)	25 543 432.7 (14)	25 543 403. (75)
B (00^00)	6081.492518 (56)	(6081.4924439)[c]
D (00^00)	1.3019369 (114) × 10^{-3}	(1.301789 × 10^{-3})[c]
B (10^00)	6063.358265 (200)	6063.3588 (8)
D (10^00)	1.329873 (197) × 10^{-3}	1.3312 (19) × 10^{-3}
H (10^00)	0.0001214 (276) × 10^{-6}	—
B (20^00)	6044.874923 (2550)	6044.891 (5)
D (20^00)	1.359731 (810) × 10^{-3}	1.3607 (10) × 10^{-3}
H (20^00)	0.0002234 (706) × 10^{-6}	—
B (01^10)	6092.078222 (289)	—
D (01^10)	1.323567 (625) × 10^{-3}	—
q (01^10)	6.361411394 (745)	—
q_J (01^10)	4.25608 (667) × 10^{-6}	—
B (11^10)	6075.50528 (186)	6075.519 (7)
D (11^10)	1.362242 (679) × 10^{-3}	—
q (11^10)	6.853553 (2121)	6.853 (13)
q_J (11^10)	11.670 (489) × 10^{-6}	—

[a] The statistically estimated uncertainties in the last digits (one standard deviation) are given in parentheses following each value. Since systematic errors have not been taken into account, these estimated uncertainties may be slightly optimistic.

[b] To convert from frequency units to wave number units, use 299 792 458 m/sec for the speed of light.[16]

[c] See Ref. 10; the negligible difference in the B_0 and D_0 values given in Ref. 10 and in this work arises from the inclusion of an H_0 term in Ref. 10.

Reference

1. J. S. Wells, F. R. Petersen, A. G. Maki, and D. J. Sukle, Appl. Opt. **20,** 1676 (1981).